Inorganica Chimica Acta 479 (2018) 128–134

Contents lists available at ScienceDirect

Inorganica Chimica Acta

journal homepage: www.elsevier.com/locate/ica

Research paper

A chromene pyrazoline derivatives fluorescent probe for Zn^{2+} detection in aqueous solution and living cells

Ying-Peng Zhang [a,*], Qing-Hua Xue [a], Yun-Shang Yang [a,*], Xiao-Yu Liu [a], Chun-Mei Ma [a], Jia-Xi Ru [b], Hui-Chen Guo [b]

[a] School of Petrochemical Engineering, Lanzhou University of Technology, Lanzhou 730050, China
[b] State Key Laboratory of Veterinary Etiological Biology and Key Laboratory of Animal Virology of Ministry of Agriculture, Lanzhou Veterinary Research Institute, Chinese Academy of Agricultural Sciences, Lanzhou 730046, China

ARTICLE INFO

Article history:
Received 23 January 2018
Received in revised form 13 April 2018
Accepted 13 April 2018
Available online 23 April 2018

Keywords:
Chromene
Pyrazoline
Fluorescent probe
Zn^{2+} recognition
Cell imaging

ABSTRACT

A new chromene pyrazoline derivatives fluorescent probe L was designed and synthesized. The probe L appears in a 55-fold fluorescence enhancement after 5 equiv. Zn^{2+} was added, and it also exhibits high sensitivity and selectivity for response to Zn^{2+} in ethanol-water (V:V = 1:1) solution through "OFF-ON" type process and a possible photoinduced electron transfer (PET). Notably, the probe L distinguishes between Zn^{2+} and Cd^{2+}. The association constant was considered as $2.38 \times 10^3\ M^{-1}$ via fluorescence titration experiments. The probe L-Zn^{2+} complex forms a 1:1 binding stoichiometry which was discussed by Job's plot. The probe is very highly sensitive with fluorometric detection limit of 1.603×10^{-10} M. It also shows good reversibility upon addition of EDTA. Furthermore, the viability of L to Zn^{2+} has practical application in live cell imaging.

1. Introduction

As we know, transition metal zinc is one of the most important in life system [1] and it is the second most rich transition metal element in the human body [2]. Zn^{2+} plays a crucial role in many biochemical processes such as cellular metabolism [3], muscle contraction [4], DNA-binding proteins [5], gene expression, apoptosis, enzyme regulation, immunity, metallo-enzyme function [6] and so forth. In pathology, Parkinson's disease [7], senile dementia [8], epilepsy disease [9], cerebral ischemia [10], diabetes [11], amyotrophic lateral sclerosis (ALS) [12], infantile diarrhea [13] and other diseases are related to the formation of Zn^{2+} and metabolic disorders. Therefore, it becomes very important to detect Zn^{2+} in both the environment and biological systems [14].

The development of fluorescent probes for Zn^{2+} detection has become a very active field in chemical biology. A lot of fluorescent probes for the detection and recognition of Zn^{2+} have been studied by various teams [15–19], but some of them can be applied only in organic solutions like acetonitrile toxic solvents, which restrict their potential applications, some of them have complex preparation process, inferior reversibility or selectivity [20–23]. In addition, some Zn^{2+} fluorescent probes display relatively low selectivity and suffer from the interferences from other metal ions, especially Cd^{2+} [24], which is the same group as Zn^{2+} in the periodic table and has similar binding properties with Zn^{2+} [25]. Therefore, similar fluorescence intensity changes and wavelength shifts are usually obtained when these two metal ions coordinate to the probe molecule respectively [26]. Thus, it is a great challenge to design and synthesize a fluorescent probe to sense and monitor Zn^{2+} with high selectivity and sensitivity in aqueous solutions [27].

In recent years, pyrazoline derivatives have drawn much attention because of their excellent blue fluorescence property, high fluorescence quantum yield, the rigid flat structure and high hole-transport efficiency [28–31].Chromene derivatives have been widely used as important intermediates in the synthesis of many natural products and medicinal agents. Many synthesized molecules based on the chromene ring system were found to be useful in antiproliferative activity [32,33]. Moreover chromone derivatives not only give fluorescence in the visible range but also cross the cell membrane very easily due to the lipophilic nature [34–38].

Chromene and pyrazoline have optical properties such as high fluorescence quantum yield, high light stability, large Stokes shift and non-toxicity. Taking all these into account, we have designed and synthesized a new compound L connecting pyrazoline ring and chromene ring. The L showed good selectivity and high sensitivity fluorescence response to Zn^{2+} over other metal ions,

* Corresponding authors.
E-mail addresses: yingpengzhang@126.com (Y.-P. Zhang), yangyunshang@tom.com (Y.-S. Yang).

https://doi.org/10.1016/j.ica.2018.04.020
0020-1693/

especially Cd^{2+} in ethanol-water (V:V = 1:1) solution. Hence, owing to the good selectivity, high sensitivity and complete reversibility for detection and recognition of Zn^{2+}, this probe L could be suitable for imaging in living cells. In contrast to previously reported Zn^{2+} fluorescent probes [39–42], the advantages of presenting new probe L are simple structure, easy synthesis, better fluorescence intensity enhancement, higher sensitivity and reversible.

2. Materials and methods

The materials used for this study were obtained from commercial suppliers and used without further purification. ^1H NMR and ^{13}C NMR spectrum were measured on the Bruker Avance 400 (400 MHz) spectrometer. Chemical shifts are reported in ppm using TMS as an internal standard. HR-ESI-MS were determined on a Bruker esquire 6000 spectrometer. UV–vis absorption spectrum were monitored with a UV-2700 spectrophotometer. Fluorescence spectrum were determined on a Hitachi F-7000 spectrophotometer equipped with quartz cuvettes of 1 cm path length. The melting point was determined on an XRC-1u Melting Point Apparatus.

Stock solution of L (1×10^{-2} M) was prepared in N, N-Dimethylformamide. Stock solutions of various metal ions (1×10^{-2} M) and EDTA (1×10^{-2} M) in distilled water were also prepared. All absorption and fluorescence emission spectrum were measured in a 1 cm optical path length quartz optical cell at room temperature. All fluorescence measurements were carried out upon excitation at 382 nm. Excitation and emission slit widths were 5.0 nm and 10.0 nm respectively.

BHK-21 cells were maintained in DMEM supplemented with 10% FBS at 37 °C under a humidified atmosphere containing 5% CO_2. Cells were plated on 18 mm glass coverslips and allowed to adhere for 24 h, treated with L (20 μM in cell culture medium), and incubated for 30 min. Subsequently, the cells were treated with Zn^{2+} (100 μM in cell culture medium). Cells were incubated for 30 min and rinsed with PBS three times to remove free compound and ions before analysis. Cells incubated with only 20 μM L for 30 min acted as a control. The cytotoxic activity experiment of the complex against BHK-21 cells was tested according to MTS assay procedures: BHK-21 cells were seeded into 96-well plates for 24 h. The different volume concentration of probe L was dissolved in DMSO make the final concentration, and diluted in culture medium at concentrations of 5, 10, 25, 50, 100 μM as working-solution and each concentration in quintuplicate, DMSO as a negative. After incubation for 24 h, the cells were added 10 μL solution of MTS in incubator for 4 h. After sufficient reaction with cells, the OD of each well was measured at the wavelength of 490 nm using a microplate spectrophotometer.

3. Experimental

The synthetic route of L (1-(3-phenyl-5-(2-phenyl-2H-chromen-3-yl)-4,5-dihydr o-1H-Pyrazol-1-yl)ethanone) was shown in Scheme 1. The probe is easy to synthesize in three steps. According to the literature [37], compound **3** readily prepared from compound **1** and **2** in 79% yield, A mixture of compound **3** (0.3384 g, 1.0 mmol) and 80% hydrazine hydrate (0.3065 g, 5.0 mmol) were taken in a 100 mL reaction flask in the presence of glacial acetic acid (15 mL) and refluxed at 120 °C for 6 h. After completion of reaction, it was cooled and poured into crushed ice. The resulting precipitate was filtered and recrystallized from ethanol to yield probe L. Pale yellow solid; Yield: 71%; mp: 216–219 °C. ^1H NMR (400 MHz, $CDCl_3$, TMS) (Fig. S1): δ_H ppm 9.98 (s, 1H), 7.40–7.27 (m, 5H), 7.17 (d, J = 5.2 Hz, 1H), 7.10–7.00 (m, 3H), 6.90 (m, 2H), 6.70–6.56 (m, 2H), 5.79 (s, 1H), 5.02 (dd, J = 7.8, 4.2 Hz, 1H), 3.45 (dd, J = 10.8, 7.8 Hz, 1H), 3.20 (dd, J = 10.8, 4.2 Hz, 1H), 1.88 (s, 3H). ^{13}C NMR (100 MHz, $CDCl_3$, TMS) (Fig. S2): δ_c ppm 167.60, 157.52, 156.20, 151.66, 138.26, 133.27, 132.28, 129.77, 129.03, 128.59, 128.24, 127.64, 126.87, 121.80, 121.21, 120.80, 119.72, 117.05, 115.96, 114.73, 77.86, 56.81, 39.60, 21.32. HR-ESI-MS (Fig. S3) calculated for $[M-H]^+$ 409.1630, found 409.2733.

Compound **6** was prepared in using the same method with probe 4. White solid; yield: 81%; mp: 136–138 °C. ^1H NMR (400 MHz, $CDCl_3$, TMS) (Fig. S4): δ_H ppm 7.67 (d, J = 5.2 Hz, 2H), 7.58–7.20 (m, 8H), 7.14–6.98 (m, 2H), 6.85 (d, J = 4.4 Hz, 1H), 6.66 (d, J = 4.8 Hz, 1H), 6.57 (s, 1H), 5.87 (s, 1H), 5.00 (d, J = 5.2 Hz, 1H), 3.32 (dd, J = 8, 11.6 Hz, 1H), 3.06 (d, J = 11.6 Hz, 1H), 2.01 (s, 3H). ^{13}C NMR (100 MHz, $CDCl_3$, TMS) (Fig. S5): 168.80, 153.92, 151.78, 138.59, 134.57, 131.10, 130.35, 129.55, 128.90, 128.73, 128.54, 127.80, 126.79, 126.45, 121.15, 121.11, 120.87, 115.93, 78.25, 58.07, 39.64, 21.36. HR-ESI-MS (Fig. S6) calculated for $[M+H]^+$ 395.1681, found 395.2558.

4. Results and discussion

4.1. Uv–vis studies of L to Zn^{2+}

The absorption spectral property of L toward different metal ions (Ag^+, Al^{3+}, Fe^{3+}, Co^{2+}, Ni^{2+}, Ba^{2+}, Ca^{2+}, Cu^{2+}, Cd^{2+}, K^+, Mg^{2+}, Na^+, Hg^{2+}, Zn^{2+}, Pb^{2+}, Li^+, Mn^{2+} all the metal ions solution was 5 equiv. of L got by dissolving their corresponding nitrate salts in H_2O) was measured in ethanol-water (V:V = 1:1). As shown in Fig. S7. L alone (10 μM) presents a broadband center at 280 nm and 320 nm. We also found that Ag^+, Al^{3+}, Co^{2+}, Ni^{2+}, Ba^{2+}, Ca^{2+}, Cd^{2+}, K^+, Mg^{2+}, Na^+, Hg^{2+}, Zn^{2+}, Pb^{2+}, Li^+, Mn^{2+} did not cause significant changes in absorption spectrums. In contrast, Cu^{2+} caused a new band at 350–430 nm and Fe^{3+} had considerable changes in absorption bands.

4.2. Fluorescence studies of L to Zn^{2+}

The fluorescence change of L with respective metal ions was monitored in ethanol-water (V:V = 1:1) solution. Among various metal ions (Ag^+, Al^{3+}, Fe^{3+}, Co^{2+}, Ni^{2+}, Ba^{2+}, Ca^{2+}, Cu^{2+}, Cd^{2+}, K^+, Mg^{2+}, Na^+, Hg^{2+}, Zn^{2+}, Pb^{2+}, Li^+ and Mn^{2+} all the metal ions solution was 5 equiv. of L), Zn^{2+} created almost 55-fold fluorescence enhancement at 471 nm(Fig. 1). And a small red shift with fluorescence enhancement was observed. The change in spectral wavelength from 441 nm to 471 nm is caused by restricted C=N isomerization mechanism and an inhibition of photo-induced electron transfer (PET) process [43,44].

Furthermore, competition experiments for other metal ions in the L-Zn^{2+} were conducted in the same condition. As displayed in Fig. 2. Hg^{2+} and Pb^{2+} can partly quench fluorescence of L-Zn^{2+}, whereas Al^{3+}, Fe^{3+} and Cu^{2+} completely quenched fluorescence of L-Zn^{2+}. This may be attributed to the paramagnetic properties of these three metal ions and fluorescence quenching was observed when complex with some paramagnetic metal ions, such as Fe^{3+} and Cu^{2+}, are always encountered in other metal ion probes [45–47]. Thus, when they were bound to probes, the emission would be strongly quenched by a photoinduced metal into fluorophore electron or energy transfer mechanism [48–51]. Most of metal ions, including Ag^+, Co^{2+}, Ni^{2+}, Ba^{2+}, Ca^{2+}, Cd^{2+}, K^+, Mg^{2+}, Na^+, Hg^{2+}, Pb^{2+}, Li^+ and Mn^{2+} show a very negligible effect, and Al^{3+}, Cu^{2+} and Fe^{3+}could quench the fluorescence, which was often encountered in other probes. This is limited to the application of probe L in complicated environment samples. However, it is surprising that L-Zn^{2+} complex eliminated the influence of Cd^{2+} by blocking PET and restricting mechanism of C=N isomerization. These results show that L strongly coordinates with Zn^{2+} which

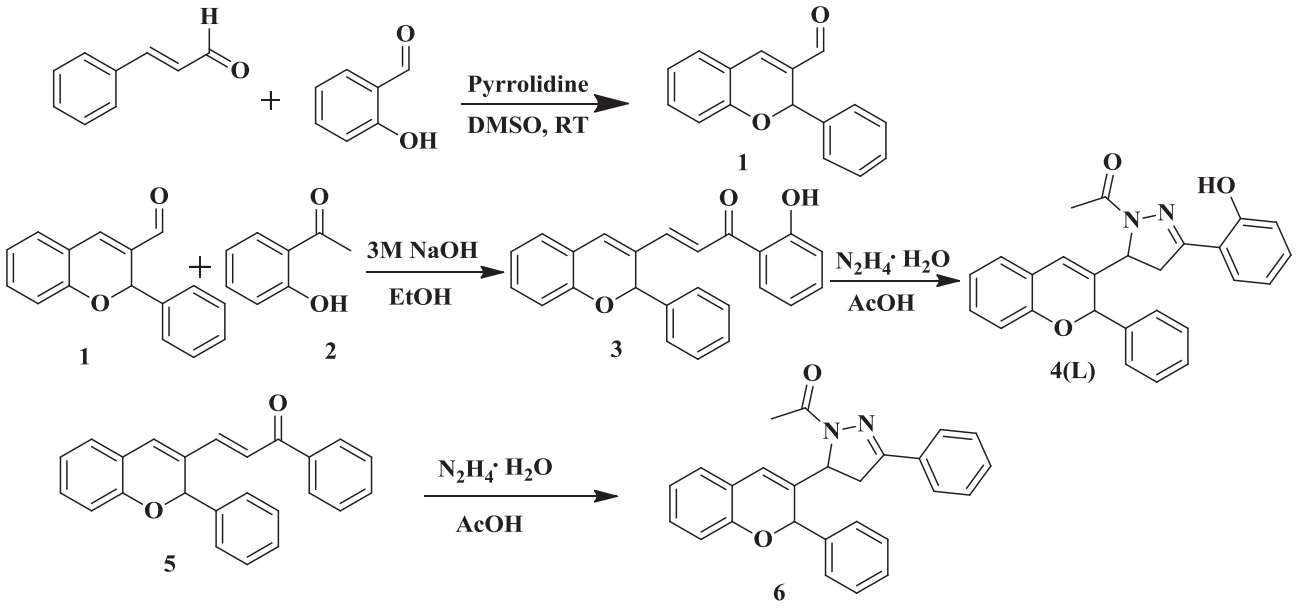

Scheme 1. Synthesis of compound **4** (L).

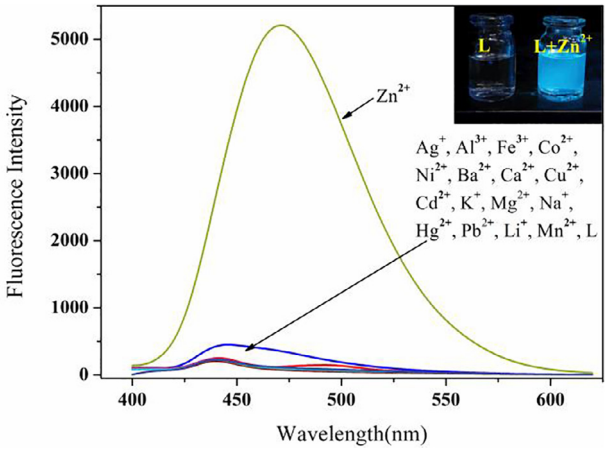

Fig. 1. Fluorescence spectra of probe L (10 μM) in ethanol–water (V:V = 1:1) solution with 5 equiv. of metal ions (λex = 382 nm, slit: 5.0/10.0 nm). Insert: Photos of L (10 μM) in ethanol–water with and without addition of Zn^{2+} (5 equiv.)

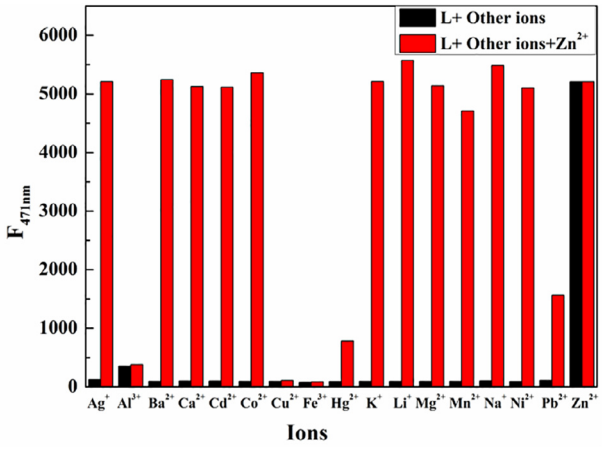

Fig. 2. Fluorescence emission spectra of L(10 μM) and Zn^{2+} (5 equiv.) in the presence of Ag^+, Al^{3+}, Ba^{2+}, Ca^{2+}, Cd^{2+}, Co^{2+}, Cu^{2+}, Fe^{3+}, Hg^{2+}, K^+, Li^+, Mg^{2+}, Mn^{2+}, Na^+, Ni^{2+}, Pb^{2+} and Zn^{2+}(5 equiv.) in ethanol–water (V:V = 1:1) solution (λex = 382 nm, slit: 5.0/10.0 nm).

could be used to distinguish Zn^{2+} from Cd^{2+} in some conditions [52].

In order to solve the sensitivity of L to Zn^{2+}, the fluorescence titration of L (10 μM) was performed with Zn^{2+} in ethanol–water (V:V = 1:1) solution (Fig. 3). L alone shows a weak fluorescence emission band at 471 nm with a rather weak fluorescence quantum yield (0.0385), when adding Zn^{2+} to L, a dramatic increase in fluorescence (fluorescence quantum yield 0.2704). And quantum yield was calculated by the general equation: $\Phi = \Phi_s(IA_s/I_sA)(\eta^2/\eta_s^2)$ [53]. With the increase addition of Zn^{2+} (0–8.5 equiv.), the fluorescent intensity was continually increased, when 6 equiv. of Zn^{2+} was added, the fluorescence intensity showed fewer enhancement. This is because that it is an equilibrium process in which excess equivalent Zn^{2+} is needed, the similar phenomenon also encountered in the other probes [18–54]. The binding rate of L-Zn^{2+} complex was studied by Job's plot methods [55] is shown in Fig. 4. The maximum mole fraction of L appears at 0.5, which supporting a 1:1 (L: Zn^{2+}) binding stoichiometry. Benesi-Hildebrand nonlinear curve fitting method is further advocated [54–56] (Fig. 5). It was found that the binding constant of L-Zn^{2+} complex is Ka = 2.38 × 10^3 M^{-1} and the limit of detection (LOD) is 1.603 × 10^{-10} M, calculated using 3σ/k (Fig. S8) [57]. Some different probes for Zn^{2+} detection were listed in the Table 1. Compared with the LOD of other probes for Zn^{2+} detection, probe L exhibits lower detection limits. The high sensitivity and low detection limit of L could be used as a trace level identification of Zn^{2+} in real level environmental samples to distinguish Zn^{2+} from Cd^{2+}. In order to further understand the binding mode of L and Zn^{2+}, we had also prepared compound **6** without a phenolic hydroxyl group. In contrast to L, compound **6** did not cause an obvious change in the presence of 5 equiv. of Zn^{2+} in ethanol-water (V:V = 1:1) solution (Fig. 6).

4.3. Reversible test of L to Zn^{2+} with EDTA

The recognition reversibility of L was further verified by fluorescence experiments with EDTA. The addition of Zn^{2+} (5 equiv.) to probe L showed that fluorescence intensity was remarkably enhanced. Upon adding EDTA (5 equiv.) to L-Zn^{2+} solution, fluores-

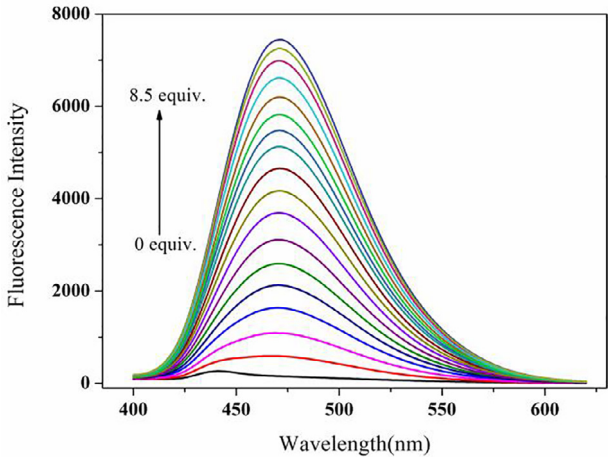

Fig. 3. Fluorescence spectra of L obtained upon addition of Zn^{2+} (0–8.5 equiv.) in ethanol–water (V:V = 1:1) solution (λex = 382 nm, slit: 5.0/10.0 nm).

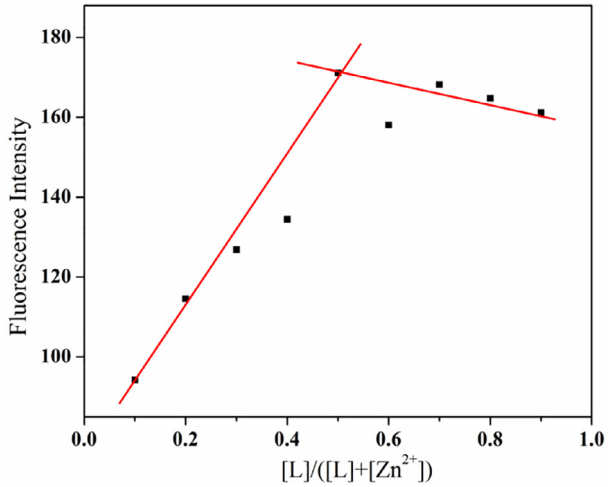

Fig. 4. Job's plot for L with Zn^{2+} ions in ethanol–water (V:V = 1:1) solution.

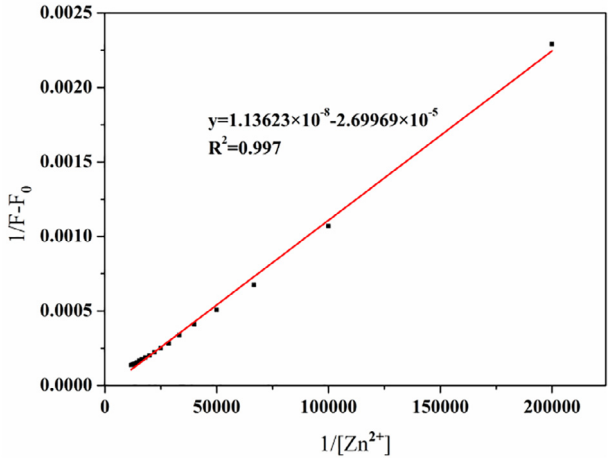

Fig. 5. Benesi-Hildebrand plot of L (10 μM) in ethanol–water (V:V = 1:1) solution in the presence of Zn^{2+} (0–8.5 equiv.). R^2 = 0.997.

cence intensity get quenched and almost reached the intensity of original receptor L because of EDTA-Zn^{2+} complex formation. This indicates that the Zn^{2+} recognition process is reversible (Fig. 7).

Table 1
LOD of other fluorescence probes (1–7) and probe L for Zn^{2+} detection.

Fluorescence probes	Ions	Detection limits
1 [58]	Zn^{2+}	8.3×10^{-7} M
2 [59]	Zn^{2+}	5.0×10^{-7} M
3 [60]	Zn^{2+}	1.23×10^{-7} M
4 [61]	Zn^{2+}	8.6×10^{-9} M
5 [52]	Zn^{2+}	2.9×10^{-9} M
6 [62]	Zn^{2+}	1.13×10^{-9} M
7 [63]	Zn^{2+}	7.5×10^{-7} M
Our probe L	Zn^{2+}	1.603×10^{-10} M

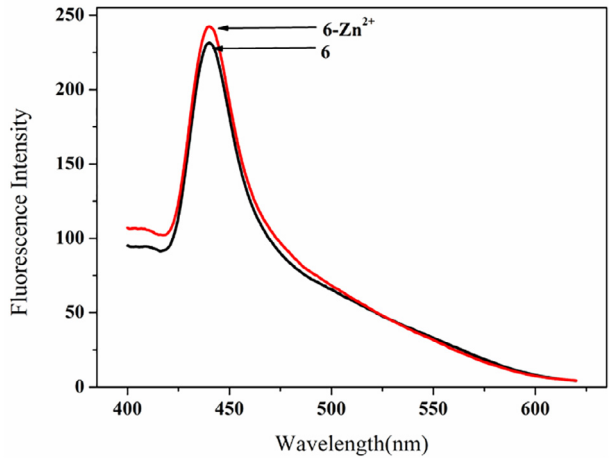

Fig. 6. Fluorescence spectra of compound **6** (1.0×10^{-5} M) in the absence and presence of 5 equiv. of Zn^{2+} in ethanol–water (V:V = 1:1) solution. (λex = 382 nm, slit: 5.0/10.0 nm).

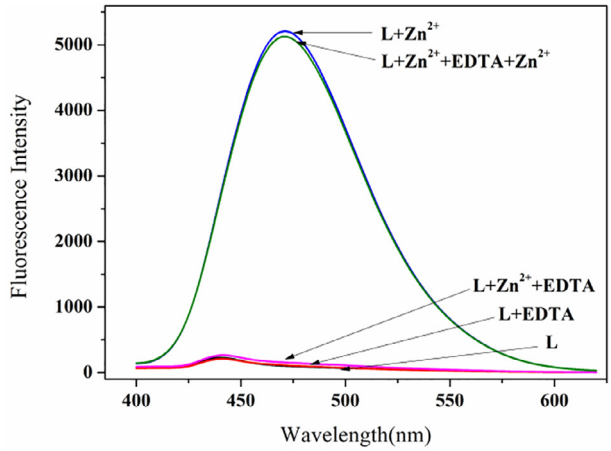

Fig. 7. Fluorescence spectra of L ((10 μM) solution (ethanol–water, V:V = 1:1) in the presence of Zn^{2+} (5 equiv.) and EDTA (5 equiv.).

4.4. Proposed mechanism of L to Zn^{2+}

The possible binding mechanism of L with Zn^{2+} induced the fluorescence changes is shown in Scheme 2. Based on the previously proposed mechanism of some reported pyrazoline-based probes [52–59], it has been possible that Zn^{2+} coordinates with the corresponding oxygen and nitrogen atoms of probe L and induces the fluorescence changes. The fluorescence enhancement was probably due to the combination of photoinduced electron transfer (PET) process and chelation-enhanced fluorescence (CHEF) [64], whereas the chelation of L with Zn^{2+} made the complex more rigid,

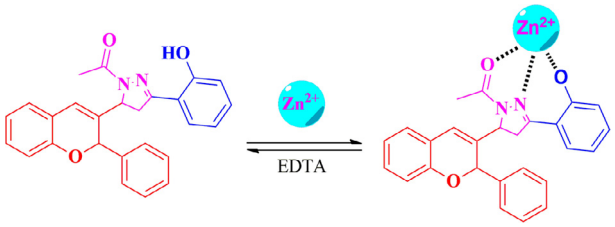

Scheme 2. Proposed binding mode of L with Zn^{2+}.

which completely restrict C=N isomerisation [65,66]. The titration studies, Job's plot and Benesi-Hildebrand nonlinear square curve fitting methods support the 1:1 binding stoichiometry of L-Zn^{2+} complex. To further understand the binding behavior of the probe L with Zn^{2+}, the ^1H NMR titration experiment was investigated. Upon addition of 0.5, 1.0, 1.5, 2.0 equiv. of Zn^{2+} to probe L in DMSO-d_6 is showed in Fig. S9, pyrazoline and aryl protons showed an upfield or downfield shift, and it is found that the hydroxyl peak at 10.04 ppm decreases and almost disappeared on addition of 1.0 equiv. of Zn^{2+}. In addition, relative changes in the ^1H NMR spectra were observed until 1.5 equiv. of Zn^{2+} was added to L, the spectra showed a slight shift upon further addition of Zn^{2+}. To provide further evidence for the binding of L with Zn^{2+}, ESI–MS spectral studies were performed. In the HR-ESI-MS spectra (Figs. S3 and S10), the probe L showed that the $[M-H]^+$ peak at 409.2733 (m/z calcd: 409.1630); however, the L-Zn^{2+} complex appeared the $[M+Zn^{2+}+H]^+$ peak at 473.2093 (m/z calcd: 474.0833), which corroborates 1:1 binding ratio for L and Zn^{2+}. The above results reveal that Zn^{2+} is coordinated with C=N, C=O and —OH groups in 1:1 binding mode.

4.5. Imaging of intracellular Zn^{2+} and cell viability of the probe

The sensitivity of L for Zn^{2+} in living BHK-21 cells was measured by fluorescence microscopy. First, BHK-21 cells incubated with the probe L were not displayed fluorescence image (Fig. 8(a)). The blue fluorescence was observed after incubation of the probe L treated cells with Zn^{2+} (Fig. 8(b)). The fluorescence images showed that

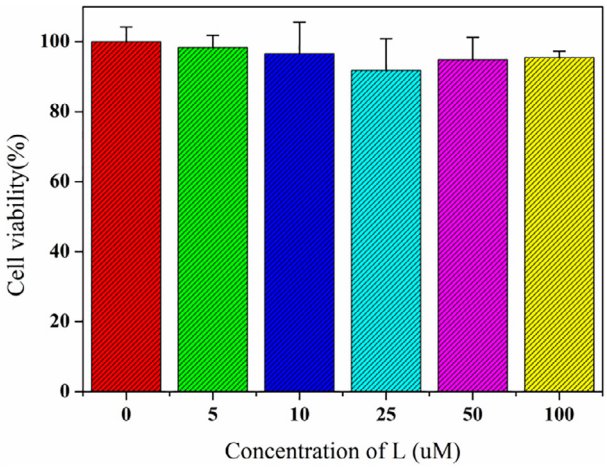

Fig. 9. Cell viability graph of probe L using BHK-21 cells by MTS assay.

the fluorescence signals are localized in the intracellular region which indicated that probe L have good cell membrane permeability. The blue significant fluorescence from the intracellular region proves that the probe L is suitable for imaging Zn^{2+} in living cells. The bioimaging in the BHK-21 cells confirmed the fluorescence enhancement with excellent cell permeability. It showed that L is biocompatible and can be used for rapid detection of intracellular Zn^{2+}. An MTS assay was used to evaluate cell viability. The viability of cells treated with the range of concentration 0–100 μM of L for 24 h was reflected in Fig. 9. The probe L is found to be least toxic to the cells.

5. Conclusion

In summary, we have designed and synthesized a new chromene-based pyrazolines fluorescent probe L for detecting Zn^{2+}. It showed that addition of Zn^{2+} increased a 55-fold fluorescence intensity compared to other metal ions particularly Cd^{2+} in ethanol-water system. The fluorescence of L-Zn^{2+} can be quenched by

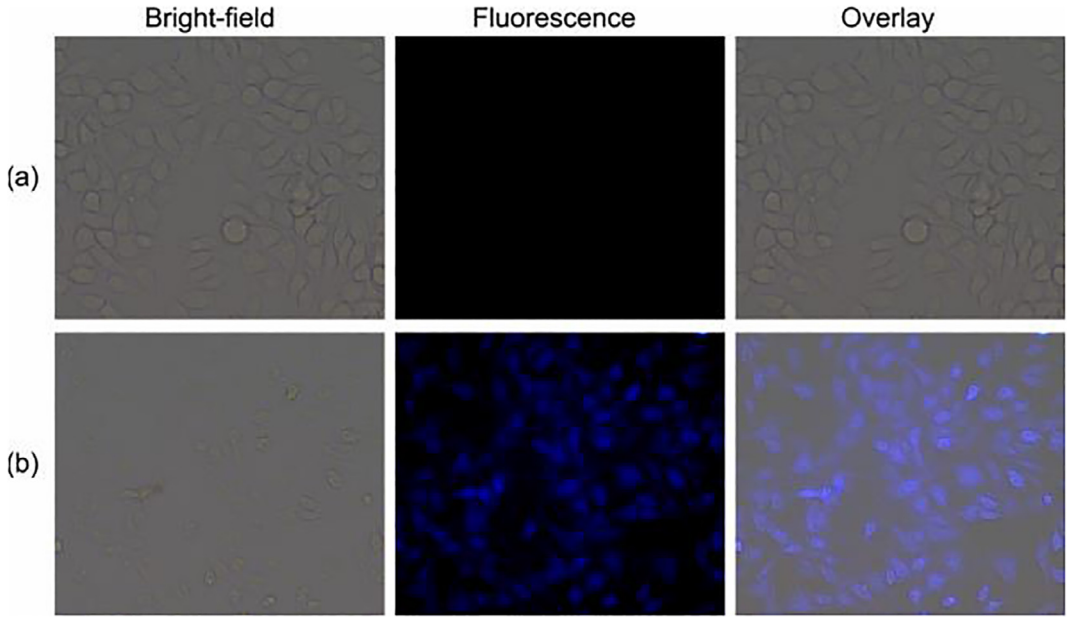

Fig. 8. Fluorescence images of BHK-21 cells. BHK-21 cells incubated with L (20 μM) for 1 h at 37 °C (a). BHK-21 cells incubated with L for 1 h and then further incubated with 100 μM Zn^{2+} for 1 h at 37 °C (b).

adding EDTA, indicating that L is a reversible probe. The binding constant of L-Zn^{2+} complex was found to be Ka = 2.38×10^3 M^{-1} and the limit of detection (LOD) is 1.603×10^{-10} M. Moreover, probe L has been used for imaging of Zn^{2+} in cells under physiological condition and shows low toxicity.

Acknowledgment

This work was supported financially by grants from the Gansu Province Natural Science Foundation of China (No. 1508RJZA078).

Appendix A. Supplementary data

Supplementary data associated with this article can be found, in the online version, at https://doi.org/10.1016/j.ica.2018.04.020.

References

[1] K.A. McCall, C.-C. Huang, C.A. Fierke, Function and mechanism of zinc metalloenzymes, J. Nutr. 130 (2000) 1437–1446.
[2] C. Andreini, L. Banci, I. Bertini, A. Rosato, Zinc through the three domains of life, J. Proteome Res. 5 (2006) 3173–3178, https://doi.org/10.1021/pr0603699.
[3] J.M. Berg, Y. Shi, The galvanization of biology: a growing appreciation for the roles of zinc, Science 271 (1996) 1081–1085, https://doi.org/10.1126/science.271.5252.1081.
[4] A.R. Kay, Imaging synaptic zinc: promises and perils, Trends Neurosci. 29 (2006) 200–206, https://doi.org/10.1016/j.tins.2006.02.004.
[5] E.L. Que, D.W. Domaille, C.J. Chang, Metals in neurobiology: probing their chemistry and biology with molecular imaging, Chem. Rev. 108 (2008) 1517–1549, https://doi.org/10.1021/cr078203u.
[6] E. Tomat, S.J. Lippard, Imaging mobile zinc in biology, Curr. Opin. Chem. Biol. 14 (2010) 225–230, https://doi.org/10.1016/j.cbpa.2009.12.010.
[7] J.H. Viles, Metal ions and amyloid fiber formation in neurodegenerative diseases. Copper, zinc and iron in Alzheimer's, Parkinson's and prion diseases, Coord. Chem. Rev. 256 (2012) 2271–2284, https://doi.org/10.1016/j.ccr.2012.05.003.
[8] N.L. Bjorklund, V.M. Sadagoparamanujam, G. Taglialatela, Selective, quantitative measurement of releasable synaptic zinc in human autopsy hippocampal brain tissue from Alzheimer's disease patients, J. Neurosci. Methods. 203 (2012) 146–151, https://doi.org/10.1016/j.jneumeth.2011.09.008.
[9] M. Seven, S.Y. Basaran, M. Cengiz, S. Unal, A. Yuksel, Deficiency of selenium and zinc as a causative factor for idiopathic intractable epilepsy, Epilepsy Res. 104 (2013) 35–39, https://doi.org/10.1016/j.eplepsyres.2012.09.013.
[10] B.G. Jang, S.J. Won, J.H. Kim, B.Y. Choi, M.W. Lee, M. Sohn, H.K. Song, S.W. Suh, EAAC1 gene deletion alters zinc homeostasis and enhances cortical neuronal injury after transient cerebral ischemia in mice, J. Trace Elem. Med Biol. 26 (2012) 85–88, https://doi.org/10.1016/j.jtemb.2012.04.010.
[11] M. Karamali, Z. Heidarzadeh, S.M. Seifati, M. Samimi, Z. Tabassi, M. Hajijafari, Z. Asemi, A. Esmaillzadeh, Zinc supplementation and the effects on metabolic status in gestational diabetes: a randomized, double-blind, placebo-controlled trial, J. Diabetes Complications 29 (2015) 1314–1319, https://doi.org/10.1016/j.jdiacomp.2015.07.001.
[12] E.J. McAllum, B.R. Roberts, J.L. Hickey, T.N. Dang, A. Grubman, P.S. Donnelly, J.R. Liddell, A.R. White, P.J. Crouch, ZnII(atsm) is protective in amyotrophic lateral sclerosis model mice via a copper delivery mechanism, Neurobiol. Dis. 81 (2015) 20–24, https://doi.org/10.1016/j.nbd.2015.02.023.
[13] H.P. Sachdev, N.K. Mittal, S.K. Mittal, H.S. Yadav, A controlled trial on utility of oral zinc supplementation in acute dehydrating diarrhea in infants, J. Pediatr. Gastroenterol. Nutr. 7 (1988) 877–881.
[14] T. Jiang, X. Xiong, S. Wang, Y. Luo, Q. Fei, A. Yu, Z. Zhu, Direct mass spectrometric analysis of zinc and cadmium in water by microwave plasma torch coupled with a linear ion trap mass spectrometer, Int. J. Mass Spectrom. 399–400 (2016) 33–39, https://doi.org/10.1016/j.ijms.2016.02.007.
[15] K. Ponnuvel, M. Kumar, V. Padmini, A new quinoline-based chemosensor for Zn^{2+} ions and their application in living cell imaging, Sensors Actuators, B Chem. 227 (2016) 242–247, https://doi.org/10.1016/j.snb.2015.12.017.
[16] K. Chantalakana, N. Choengchan, P. Yingyuad, P. Thongyoo, A highly selective "turn-on" fluorescent sensor for Zn^{2+} based on fluorescein conjugates, Tetrahedron Lett. 57 (2016) 1146–1149, https://doi.org/10.1016/j.tetlet.2016.01.106.
[17] J.-H. Hu, J.-B. Li, J. Qi, Y. Sun, Acylhydrazone based fluorescent chemosensor for zinc in aqueous solution with high selectivity and sensitivity, Sensors Actuators B Chem. 208 (2015) 581–587, https://doi.org/10.1016/j.snb.2014.11.066.
[18] Z. Dong, Y. Guo, X. Tian, J. Ma, Quinoline group based fluorescent sensor for detecting zinc ions in aqueous media and its logic gate behaviour, J. Lumin. 134 (2013) 635–639, https://doi.org/10.1016/j.jlumin.2012.07.016.
[19] W. Wang, R. Li, T. Song, C. Zhang, Y. Zhao, Study on the fluorescent chemosensors based on a series of bis-Schiff bases for the detection of zinc (II), Spectrochim. Acta - Part A Mol. Biomol Spectrosc. 164 (2016) 133–138, https://doi.org/10.1016/j.saa.2016.04.016.
[20] Z.L. Gong, B.X. Zhao, W.Y. Liu, H.S. Lv, A new highly selective "turn on" fluorescent sensor for zinc ion based on a pyrazoline derivative, J. Photochem. Photobiol. A Chem. 218 (2011) 6–10, https://doi.org/10.1016/j.jphotochem.2010.11.014.
[21] H. Mu, R. Gong, Q. Ma, Y. Sun, E. Fu, A novel colorimetric and fluorescent chemosensor: synthesis and selective detection for Cu^{2+} and Hg^{2+}, Tetrahedron Lett. 48 (2007) 5525–5529, https://doi.org/10.1016/j.tetlet.2007.05.155.
[22] C. Kiran Kumar, R. Trivedi, L. Giribabu, S. Niveditha, K. Bhanuprakash, B. Sridhar, Ferrocenyl pyrazoline based multichannel receptors for a simple and highly selective recognition of Hg^{2+} and Cu^{2+} ions, J. Organomet. Chem. 780 (2015) 20–29, https://doi.org/10.1016/j.jorganchem.2014.12.027.
[23] W. Tan, T. Leng, G. Lai, Z. Li, K. Wang, Y. Shen, C. Wang, A novel coumarin-based fluorescence enhancement and colorimetric probe for Cu^{2+}via selective hydrolysis reaction, J. Photochem. Photobiol. A Chem. 324 (2016) 81–86, https://doi.org/10.1016/j.jphotochem.2016.03.014.
[24] C. Gao, X. Jin, X. Yan, P. An, Y. Zhang, L. Liu, H. Tian, W. Liu, X. Yao, Y. Tang, A small molecular fluorescent sensor for highly selectivity of zinc ion, Sensors Actuators, B Chem. 176 (2013) 775–781, https://doi.org/10.1016/j.snb.2012.09.052.
[25] H. Ming, R. Naidu, B. Sarkar, D.T. Lamb, Y. Liu, M. Megharaj, D. Sparks, Competitive sorption of cadmium and zinc in contrasting soils, Geoderma 268 (2016) 60–68, https://doi.org/10.1016/j.geoderma.2016.01.021.
[26] J. Cherif, N. Derbel, M. Nakkach, H. Von Bergmann, F. Jemal, Z. Ben Lakhdar, Spectroscopic studies of photosynthetic responses of tomato plants to the interaction of zinc and cadmium toxicity, J. Photochem. Photobiol. B Biol. 111 (2012) 9–16, https://doi.org/10.1016/j.jphotobiol.2012.03.002.
[27] M. Ozdemir, A selective fluorescent "turn-on" sensor for recognition of Zn^{2+} in aqueous media,, Spectrochim. Acta - Part A Mol. Biomol Spectrosc. 161 (2016) 115–121, https://doi.org/10.1016/j.saa.2016.02.040.
[28] J. Li, D. Li, Y. Han, S. Shuang, C. Dong, Synthesis of 1-phenyl-3-biphenyl-5-(N-ethylcarbazole-3-yl)-2-pyrazoline and its use as DNA probe, Spectrochim. Acta Part A Mol. Biomol. Spectrosc. 73 (2009) 221–225, https://doi.org/10.1016/j.saa.2009.01.019.
[29] M.M. Li, S.Y. Huang, H. Ye, F. Ge, J.Y. Miao, B.X. Zhao, A new pyrazoline-based fluorescent probe for Cu^{2+} in live cells, J. Fluoresc. 23 (2013) 799–806, https://doi.org/10.1007/s10895-013-1203-0.
[30] Z. Zhang, F.-W. Wang, S.-Q. Wang, F. Ge, B.-X. Zhao, J.-Y. Miao, A highly sensitive fluorescent probe based on simple pyrazoline for Zn^{2+} in living neuron cells, Org. Biomol. Chem. 10 (2012) 8640, https://doi.org/10.1039/c2ob26375k.
[31] Z.L. Gong, F. Ge, B.X. Zhao, Novel pyrazoline-based selective fluorescent sensor for Zn^{2+} in aqueous media, Sensors Actuators, B Chem. 159 (2011) 148–153, https://doi.org/10.1016/j.snb.2011.06.064.
[32] W.W. Mao, T.T. Wang, H.P. Zeng, Z.Y. Wang, J.P. Chen, J.G. Shen, Synthesis and evaluation of novel substituted 5-hydroxycoumarin and pyranocoumarin derivatives exhibiting significant antiproliferative activity against breast cancer cell lines, Bioorg. Med. Chem. Lett. 19 (2009) 4570–4573, https://doi.org/10.1016/j.bmcl.2009.06.098.
[33] K.V. Sashidhara, J.N. Rosaiah, M. Kumar, R.K. Gara, L.V. Nayak, K. Srivastava, H. K. Bid, R. Konwar, Neo-tanshinlactone inspired synthesis, in vitro evaluation of novel substituted benzocoumarin derivatives as potent anti-breast cancer agents, Bioorg. Med. Chem. Lett. 20 (2010) 7127–7131, https://doi.org/10.1016/j.bmcl.2010.09.040.
[34] L. Abrunhosa, M. Costa, F. Areias, A. Venâncio, F. Proença, Antifungal activity of a novel chromene dimer, J. Ind. Microbiol.Biotechnol. 34 (2007) 787–792, https://doi.org/10.1007/s10295-007-0255-z.
[35] I. Kostova, Synthetic and natural coumarins as antioxidants, Mini Rev. Med. Chem. 6 (2006) 365–374, https://doi.org/10.2174/138955706776361457.
[36] K. Asres, A. Seyoum, C. Veeresham, F. Bucar, S. Gibbons, Naturally derived anti-HIV agents, Phyther. Res. 19 (2005) 557–581, https://doi.org/10.1002/ptr.1629.
[37] S. Nayak, S. Chakroborty, S. Bhakta, P. Panda, S. Mohapatra, S. Kumar, P. Jena, C. Purohit, Design and synthesis of (*E*)-4-(2-phenyl-2*H*-chromen-3-yl)but-3-en-2-ones and evaluation of their *in vitro* antimicrobial activity, Lett. Org. Chem. 12 (2015) 352–358, https://doi.org/10.2174/1570178612666150331204016.
[38] E.N. Kaya, F. Yuksel, G.A. Özpinar, M. Bulut, M. Durmuş, 7-Oxy-3-(3,4,5-trimethoxyphenyl)coumarin substituted phthalonitrile derivatives as fluorescent sensors for detection of Fe^{3+} ions: experimental and theoretical study, Sensors Actuators, B Chem. 194 (2014) 377–388, https://doi.org/10.1016/j.snb.2013.12.044.
[39] X.Y. Chen, J. Shi, Y.M. Li, F.L. Wang, X. Wu, Q.X. Guo, L. Liu, Two-photon fluorescent probes of biological Zn(II) derived from 7-hydroxyquinoline, Org. Lett. 11 (2009) 4426–4429, https://doi.org/10.1021/ol901787w.
[40] Z. Xu, K.H. Baek, H.N. Kim, J. Cui, X. Qian, D.R. Spring, I. Shin, J. Yoon, Zn^{2+}-triggered amide tautomerization produces a highly Zn^{2+}-selective, cell-permeable, and ratiometric fluorescent sensor, J. Am. Chem. Soc. 132 (2010) 601–610, https://doi.org/10.1021/ja907334j.
[41] L. Tang, X. Dai, K. Zhong, D. Wu, X. Wen, A novel 2,5-diphenyl-1,3,4-oxadiazole derived fluorescent sensor for highly selective and ratiometric recognition of Zn^{2+} in water through switching on ESIPT, Sensors Actuators, B Chem. 203 (2014) 557–564, https://doi.org/10.1016/j.snb.2014.07.022.

[42] P.K. Mehta, E.T. Oh, H.J. Park, K.H. Lee, Ratiometric fluorescent probe based on symmetric peptidyl receptor with picomolar affinity for Zn^{2+} in aqueous solution, Sensors Actuators, B Chem. 245 (2017) 996–1003, https://doi.org/10.1016/j.snb.2017.01.154.
[43] S. Santhoshkumar, K. Velmurugan, J. Prabhu, G. Radhakrishnan, R. Nandhakumar, A naphthalene derived Schiff base as a selective fluorescent probe for Fe^{2+}, Inorg. Chim. Acta. 439 (2016) 1–7, https://doi.org/10.1016/j.ica.2015.09.030.
[44] K. Velmurugan, R. Nandhakumar, Binol based "turn on" fluorescent chemosensor for mercury ion, J. Lumin. 162 (2015) 8–13, https://doi.org/10.1016/j.jlumin.2015.01.039.
[45] H.-Y. Lin, P.-Y. Cheng, C.-F. Wan, A.-T. Wu, A turn-on and reversible fluorescence sensor for zinc ion, Analyst 137 (2012) 4415, https://doi.org/10.1039/c2an35752f.
[46] A. Misra, M. Shahid, P. Srivastava, Optoelectronic behavior of bischromophoric dyads exhibiting Zn^{2+}/F^- ions induced "turn-On/Off" fluorescence, Sensors Actuators, B Chem. 169 (2012) 327–340, https://doi.org/10.1016/j.snb.2012.05.006.
[47] L. Xue, C. Liu, H. Jiang, Highly sensitive and selective fluorescent sensor for distinguishing cadmium from zinc ions in aqueous media, Org. Lett. 11 (2009) 1655–1658, https://doi.org/10.1021/ol900315r.
[48] L. Wannasen, E. Swatsitang, Magnetic properties dependence on Fe^{2+}/Fe^{3+} and oxygen vacancies in $SrTi_{0.95}Fe_{0.05}O_3$ nanocrystalline prepared by hydrothermal method, Microelectron. Eng. 146 (2015) 92–98, https://doi.org/10.1016/j.mee.2015.04.119.
[49] T. Fichtner, G. Kreiner, S. Chadov, G.H. Fecher, W. Schnelle, A. Hoser, C. Felser, Magnetic and transport properties in the Heusler series $Ni_{2-x}Mn_{1+x}Sn$ affected by chemical disorder, Intermetallics 57 (2015) 101–112, https://doi.org/10.1016/j.intermet.2014.10.012.
[50] Y.Z. Voloshin, A.Y. Lebedev, V.V. Novikov, A.V. Dolganov, A.V. Vologzhanina, E. G. Lebed, A.A. Pavlov, Z.A. Starikova, M.I. Buzin, Y.N. Bubnov, Template synthesis, X-ray structure, spectral and redox properties of the paramagnetic alkylboron-capped cobalt(II) clathrochelates and their diamagnetic iron(II)-containing analogs, Inorganica Chim. Acta. 399 (2013) 67–78, https://doi.org/10.1016/j.ica.2012.12.042.
[51] A.M. Elshahawy, M.H. Mahmoud, S.A. Makhlouf, H.H. Hamdeh, Role of Cu^{2+} substitution on the structural and magnetic properties of Ni-ferrite nanoparticles synthesized by the microwave-combustion method, Ceram. Int. 41 (2015) 11264–11271, https://doi.org/10.1016/j.ceramint.2015.05.079.
[52] G. Kasirajan, V. Krishnaswamy, N. Raju, M. Mahalingam, M. Sadasivam, M. Palathurai Subramaniam, S. Ramasamy, New pyrazolo-quinoline scaffold as a reversible colorimetric fluorescent probe for selective detection of Zn^{2+} ions and its imaging in live cells, J. Photochem. Photobiol. A Chem. 341 (2017) 136–145, https://doi.org/10.1016/j.jphotochem.2017.03.035.
[53] S. Song, D. Ju, J. Li, D. Li, Y. Wei, C. Dong, P. Lin, S. Shuang, Synthesis and spectral characteristics of two novel intramolecular charge transfer fluorescent dyes, Talanta 77 (2009) 1707–1714, https://doi.org/10.1016/j.talanta.2008.10.008.
[54] J. Prabhu, K. Velmurugan, R. Nandhakumar, Development of fluorescent lead II sensor based on an anthracene derived chalcone, Spectrochim. Acta - Part A Mol. Biomol Spectrosc. 144 (2015) 23–28, https://doi.org/10.1016/j.saa.2015.02.028.
[55] L. Tang, N. Wang, Q. Zhang, J. Guo, R. Nandhakumar, A new benzimidazole-based quinazoline derivative for highly selective sequential recognition of Cu^{2+} and CN^-, Tetrahedron Lett. 54 (2013) 536–540, https://doi.org/10.1016/j.tetlet.2012.11.078.
[56] F. Wang, R. Nandhakumar, J.H. Moon, K.M. Kim, J.Y. Lee, J. Yoon, Ratiometric fluorescent chemosensor for silver ion at physiological pH, Inorg. Chem. 50 (2011) 2240–2245, https://doi.org/10.1021/ic1018967.
[57] K. Velmurugan, S. Suresh, S. Santhoshkumar, M. Saranya, R. Nandhakumar, A simple Chalcone-based ratiometric chemosensor for silver ion, Luminescence 31 (2016) 722–727, https://doi.org/10.1002/bio.3016.
[58] T.T. Zhang, F.W. Wang, M.M. Li, J.T. Liu, J.Y. Miao, B.X. Zhao, A simple pyrazoline-based fluorescent probe for Zn^{2+} in aqueous solution and imaging in living neuron cells, Sensors Actuators, B Chem. 186 (2013) 755–760, https://doi.org/10.1016/j.snb.2013.06.085.
[59] M.M. Li, F.W. Wang, X.Y. Wang, T.T. Zhang, Y. Xu, Y. Xiao, J.Y. Miao, B.X. Zhao, A new turn-on fluorescence probe for Zn^{2+} in aqueous solution and imaging application in living cells, Anal. Chim. Acta. 826 (2014) 77–83, https://doi.org/10.1016/j.aca.2014.04.001.
[60] T.-T. Zhang, X.-P. Chen, J.-T. Liu, L.-Z. Zhang, J.-M. Chu, L. Su, B.-X. Zhao, A high sensitive fluorescence turn-on probe for imaging Zn^{2+} in aqueous solution and living cells, RSC Adv. 4 (2014) 16973–16978, https://doi.org/10.1039/c4ra00584h.
[61] M. Kumar, A. Kumar, M.K. Singh, S.K. Sahu, R.P. John, A novel benzidine based Schiff base "turn-on" fluorescent chemosensor for selective recognition of Zn^{2+}, Sensors Actuators, B Chem. 241 (2017) 1218–1223, https://doi.org/10.1016/j.snb.2016.10.008.
[62] L.-M. Pu, S.F. Akogun, X.-L. Li, H.-T. Long, W.-K. Dong, Y. Zhang, A Salamo-type fluorescent sensor for selective detection of Zn^{2+}/Cu^{2+} and its novel Cd^{2+} complex with triangular prism geometry, Polyhedron 134 (2017) 356–364, https://doi.org/10.1016/j.poly.2017.06.038.
[63] Y. Jin, S. Wang, Y. Zhang, B. Song, Highly selective fluorescent chemosensor based on benzothiazole for detection of Zn^{2+}, Sensors Actuators, B Chem. 225 (2016) 167–173, https://doi.org/10.1016/j.snb.2015.11.039.
[64] Y. Mikata, A. Yamashita, A. Kawamura, H. Konno, Y. Miyamoto, S. Tamotsu, Bisquinoline-based fluorescent zinc sensors, Dalt. Trans. (2009) 3800, https://doi.org/10.1039/b820763a.
[65] D. Maity, T. Govindaraju, Naphthaldehyde-urea/thiourea conjugates as turn-on fluorescent probes for Al^{3+} based on restricted C=N isomerization, Eur. J. Inorg. Chem. (2011) 5479–5485, https://doi.org/10.1002/ejic.201100772.
[66] K. Velmurugan, A. Raman, S. Easwaramoorthi, R. Nandhakumar, Pyrene pyridine-conjugate as Ag selective fluorescent chemosensor, RSC Adv. 4 (2014) 35284–35289, https://doi.org/10.1039/C4RA04001E.